Accepted Manuscript

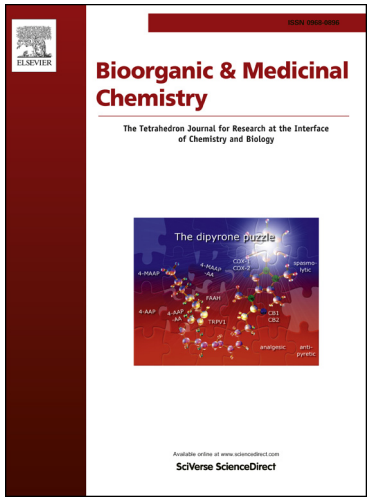

Pyrazole clubbed triazolo[1,5-*a*]pyrimidine hybrids as an anti-tubercular agents: Synthesis, in vitro screening and molecular docking study

Jaimin D. Bhatt, Chaitanya J. Chudasama, Kanuprasad D. Patel

PII: S0968-0896(15)30143-7
DOI: http://dx.doi.org/10.1016/j.bmc.2015.11.018
Reference: BMC 12666

To appear in: *Bioorganic & Medicinal Chemistry*

Received Date: 11 September 2015
Revised Date: 6 November 2015
Accepted Date: 16 November 2015

Please cite this article as: Bhatt, J.D., Chudasama, C.J., Patel, K.D., Pyrazole clubbed triazolo[1,5-*a*]pyrimidine hybrids as an anti-tubercular agents: Synthesis, in vitro screening and molecular docking study, *Bioorganic & Medicinal Chemistry* (2015), doi: http://dx.doi.org/10.1016/j.bmc.2015.11.018

Graphical Abstract

To create your abstract, type over the instructions in the template box below.
Fonts or abstract dimensions should not be changed or altered.

Pyrazole clubbed triazolo[1,5-*a*]pyrimidine hybrids as an anti-tubercular agents: Synthesis, in vitro screening and molecular docking study

Leave this area blank for abstract info.

Jaimin D. Bhatt[1], Chaitanya J. Chudasama[2], Kanuprasad D. Patel[1*]
[1]*Chemistry Department, V. P. & R. P. T. P. Science College, Affiliated to Sardar Patel University, Vallabh Vidyanagar-388 120, Gujarat, India.*
[2]*Department of Biochemistry, Shree Alpesh N. Patel P. G. Institute, Affiliated to Sardar Patel University, Anand-388001, Gujarat, India.*

MIC: 0.39 μM

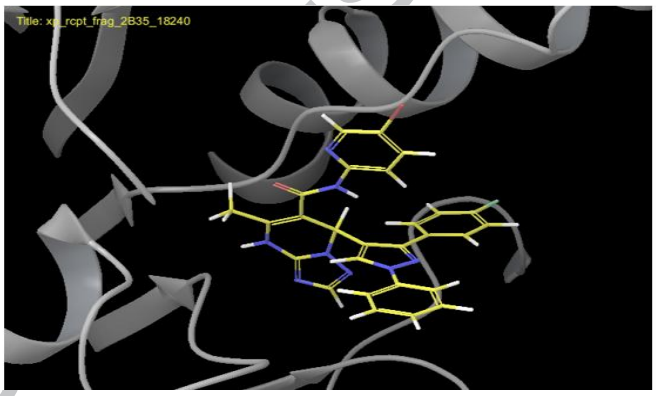

Bioorganic & Medicinal Chemistry
journal homepage: www.elsevier.com

Pyrazole clubbed triazolo[1,5-*a*]pyrimidine hybrids as an anti-tubercular agents: Synthesis, in vitro screening and molecular docking study

Jaimin D. Bhatt [a], Chaitanya J. Chudasama [b], Kanuprasad D. Patel [a*]

[a]*Chemistry Department, V. P. & R. P. T. P. Science College, Affiliated to Sardar Patel University, Vallabh Vidyanagar-388120, Gujarat, India.*
[b]*Department of Biochemistry, Shree Alpesh N. Patel P. G. Institute, Affiliated to Sardar Patel University, Anand-388001, Gujarat, India.*

ARTICLE INFO

Article history:
Received
Received in revised form
Accepted
Available online

Keywords:
Triazolopyrimidine
Diaryl pyrazole aldehydes
Glide
Enzyme inhibition assay
ADME

ABSTRACT

A series of novel pyrazole linked triazolo-pyrimidine hybrids were synthesized and evaluated for their anti-tuberculosis activity against *M.tb* H37Rv strain. Some of the screened entities rendered promising anti-*tb* activity (MIC: 0.39 µg/mL) and were found non toxic against Vero cells (IC_{50}: ≥20 µg/mL). Further, the docking study against wild type InhA enzyme of *M. tuberculosis* using Glide reproduced the most active inhibitors (**J21** & **J27**) with lowest binding energies and highest Glide XP scores demonstrating efficient binding to the active pocket. Additionally, the enzyme inhibition assay and ADME prediction of the active proved to be an attest to the possibility of developing compound **J27** as a potent anti-tubercular lead.

1. Introduction

Tuberculosis (Tb) which is mainly caused by *Mycobacterium Tuberculosis* (*M.tb*), is still throned a devastating threat across the globe.[1] Despite of having acute antitubercular chemotherapy, over 2 million new cases are reported every year.[2] The drug resistance surveillance data indicated 0.5 million new cases of multidrug resistance Tb (MDR-Tb) during the year 2013.[3] The increasing multidrug resistance among the pathogens has urged the urgency for development of new agents that can shorter the lengthy Tb therapy as well as inhibits the targets involved in persistency or dormancy.[4]

On vantage point of drug discovery and medicinal chemistry, choice of the proteins involved in regulatory functions as an inhibitory target is a crux of matter in drug development regime. In the case of *Mycobacterium*, FAS-II co-exists with the type I (FAS-I) pathway, a situation that is unique to this genus. Here FAS-I is responsible for *de novo* synthesis leading to C16–C26 fatty acids, which are used for production of phospholipids and as primers for complex lipids. The FAS-II system here in extends these fatty acids up to C56 making the long chain precursors which are required for the synthesis of cell wall-associated mycolic acids that are specific to Mycobacteria.[5] The cell wall of *M.tb* comprises of mycolic acids covalently linked to arabinogalactam, which provide complex mycobacterial envelope eliciting the ability to prevail against the chemical injuries.[5] Protein enoyl acyl carrier protein (ACP) reductase (InhA) plays a catalytic role in final step of fatty acid elongation pathway and is also a target for the activated form of Isoniazide (INH), a half century old drug.[6]

Heterocyclic and fused heterocyclic compounds are ubiquitous and plays vital role in metabolism of all living cells.[7] A class of fused heterocyclic entity is bridge headed nitrogen containing triazolopyrimidine derivatives, resembling to purine has remarkable therapeutic and pharmacological applications.[8] They are functional therapeutics, especially for the treatment and prevention of cardiovascular diseases, also known to posses smooth muscles cell growth inhibiting efficacy, are efficient analgesics and anti inflammatory agents.[9] Another class of heterocyclic entities, pyrazole derivative occurs in many drugs and synthetic products. Synthetic analogues of pyrazole are known to show phenomenal antitubercular activity especially 1,3-diphenyl pyrazole motif is known to be potent antituberculosis agent.[10,11] The carboxamide side chain has shown enhancement in the pharmacological output of pyrimidine as parent motif[11] and further it was noted that replacement of benzene by pyridine ring augmented fungicidal, antibacterial and anticancer activities.[12a] Moreover, the pyrazole and carboxamide derivatives are reported to owe potent InhA direct inhibitory activity both *in vitro* and *in vivo*.[12b]

∗ Corresponding author. Tel.: +91 2692-230011; fax: +91-2692-235207; e-mail: drkdpatel64@yahoo.co.in (KD Patel); jaiminbhatt1488@gmail.com (JD Bhatt)

Scrutinizing the above implications, we here in developed hybrid 1-3 diarylpyrazole ligated triazolopyrimidines possessing pyridyl carboxamide moieties. The developed hybrid molecules were screened for their antituberculosis activity against H37Rv strain of *M. tuberculosis*. Furthermore, docking studies and ADME prediction were carried out computationally to get insight of the structural parameters leading to activity.

2. Result and Discussion

2.1. Chemistry

The conjectured target triazolopyrimidine derivatives (J1-J30) were obtained in single step by multicomponent amalgamation of pyridin-2-*yl*-3-oxobutanamide derivatives, 1,3-diphenyl-1*H*-pyrazole-4-carbaldehyde derivatives and amino-triazole (1.5 equivalent) in appropriate quantity using dimethylformamide as reaction medium under refluxing condition as delineated in Scheme 1. The one pot reaction methodology adopted to obtain the final hybrid 7-(1,3-diphenyl-pyrazol-4-*yl*)-5-methyl-*N*-(pyridin-2-*yl*)-4,7-dihydro[1,2,4] triazolo[1,5-*a*]pyrimidine-6-carboxamide in good yields.

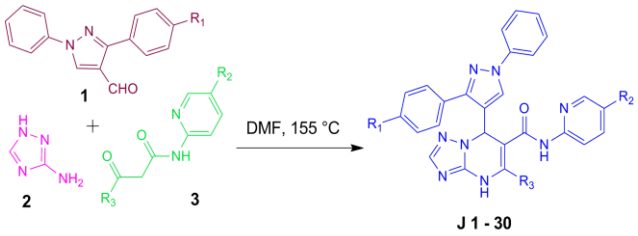

Scheme 1: Synthesis of triazolopyrimidines **J1-J30**; Reagent and Conditions: DMF, reflux

The formation of triazolopyrimidines was confirmed by observing the characteristic spectral data of the synthesized compounds **J1-J30** which were fully in agreement with their proposed structures. FT-IR results also indicates the conformation of the synthesized compound by peculiar band of amide as well as amine at 3419-3372 cm^{-1}, also a band at ~1566 cm^{-1} indicates C=N stretching of triazole ring and a band at 1697-1657 cm^{-1} corresponds to C=O stretching of amide linkage. Two medium bands observed at 2978-2950 and 2941-2899 cm^{-1} corresponds to asymmetrical and symmetrical stretching of methyl group. All the entitled motifs showed a singlet of asymmetric CH proton in ^{1}H NMR spectrum between 6.20-5.94 δ ppm, a singlet for the methine proton of triazole ring at ~7.65 δ ppm, singlets for amino as well as amide group protons at 10.12-9.95 and 10.63-10.39 δ ppm, respectively. A singlet was observed at 2.17-2.08 corresponding to methyl group at C2 position of triazolopyrimidine ring, characteristic multiplet and two singlets were observed at ~3.9, 1.24-1.07 and 1.16-1.06 respectively corresponding to isopropyl group of triazolopyrimidine ring. The aromatic ring protons and J value were found to be in accordance with substitution pattern on phenyl ring. All the final products were also confirmed by performing ESI-MS and observing the molecular ion peak.

2.2. In-vitro antituberculosis activity

The synthesized compounds **J1-J30** were evaluated for their anti-*tb* potency against *M.tb* H37Rv strain (MTCC 300) using LJ medium and broth dilution technique. Preliminary screening was carried out at 6.25 µg/mL concentration and the compounds exhibiting more than or equal to 90% inhibition in the initial screen were retested at and below 6.25 µg/mL using twofold dilution to determine the actual MIC. In the preliminary screening compounds **J3**, **J15**, **J21**, **J25** and **J27** inhibited *M. tb* in range of 90-100% as summarized in Table 1. Further, the secondary screening results represented that two compounds (**J3** & **J15**) inhibited the mycobacterium strain at MIC 3.13 µg/mL and 1.56 µg/mL, while the three compounds (**J21**, **J25** & **J27**) inhibited *M. tb* at MIC lower than 1 µg/mL. These results revealed that the compounds demonstrate moderate activity as compared to Isoniazide but good activity against *M. tb* as compared to Ethambutol and Rifampicin.

Table 1: *In-vitro* anti-tuberculosis activity and cytotoxicity of triazolo-pyrimidine hybrids

Compound	R_1	R_2	R_3	% Inhibition (at 6.25 µg /mL)	MIC µg/mL
J1	H	H	Me	72	N.D.
J2	H	CH_3	Me	66	N.D.
J3	H	Br	Me	95	3.13 ±0.313
J4	H	H	*i*-Pr	45	N.D.
J5	H	CH_3	*i*-Pr	42	N.D.
J6	H	Br	*i*-Pr	54	N.D.
J7	Me	H	Me	56	N.D.
J8	Me	CH_3	Me	49	N.D.
J9	Me	Br	Me	64	N.D.
J10	Me	H	*i*-Pr	55	N.D.
J11	Me	CH_3	*i*-Pr	46	N.D.
J12	Me	Br	*i*-Pr	66	N.D.
J13	NO_2	H	Me	84	N.D.
J14	NO_2	CH_3	Me	68	N.D.
J15	NO_2	Br	Me	96	1.56 ± 0.083
J16	NO_2	H	*i*-Pr	74	N.D.
J17	NO_2	CH_3	*i*-Pr	68	N.D.
J18	NO_2	Br	*i*-Pr	78	N.D.
J19	Cl	H	Me	84	N.D.
J20	Cl	CH_3	Me	79	N.D.
J21	Cl	Br	Me	98	0.78 ±0.039
J22	Cl	H	*i*-Pr	81	N.D.
J23	Cl	CH_3	*i*-Pr	76	N.D.
J24	Cl	Br	*i*-Pr	84	N.D.
J25	F	H	Me	99	0.78 ±0.039
J26	F	CH_3	Me	86	N.D.
J27	F	Br	Me	99	0.39 ± 0.019
J28	F	H	*i*-Pr	84	N.D.
J29	F	CH_3	*i*-Pr	82	N.D.
J30	F	Br	*i*-Pr	88	N.D.
INH	--	--	--	99	0.3
Rifampicin	--	--	--	99	0.5
Ethambutol	--	--	--	99	3.125

ND denotes Not determined, Minimum inhibitory concentration (MIC) against H37Rv strain of M. tuberculosis (µg/mL).

The substitutional pattern at three positions R_1, R_2 and R_3 of the hybrid molecules were studied for their effect on anti-tuberculosis efficacy. It emerged out that substitution at position R_1 of aryl ring of pyrazole demonstrated maximum effect on the

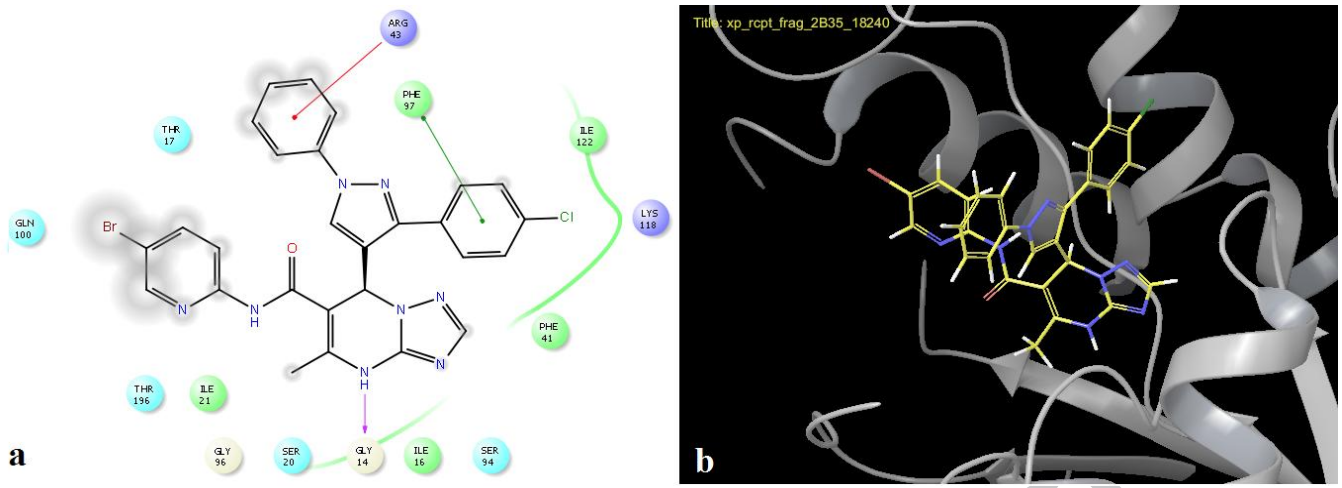

activity pattern of the hybrid molecule. The electron withdrawing group (–F, –Cl, $–NO_2$) enhanced the activity of the compounds (**J15**, **J21**, **J25** & **J27**), whereas methyl group at this position

Figure 1: The binding model of docked compound **J21** with enoyl ACP reductase (InhA) enzyme. The enzyme is displayed as cartoon, while the compounds as stick model. **(a)** 2D model enumerating the interactions of the ligand **J21** with the enzyme **(b)** 3D model of compound **J21** in the binding pocket of InhA.

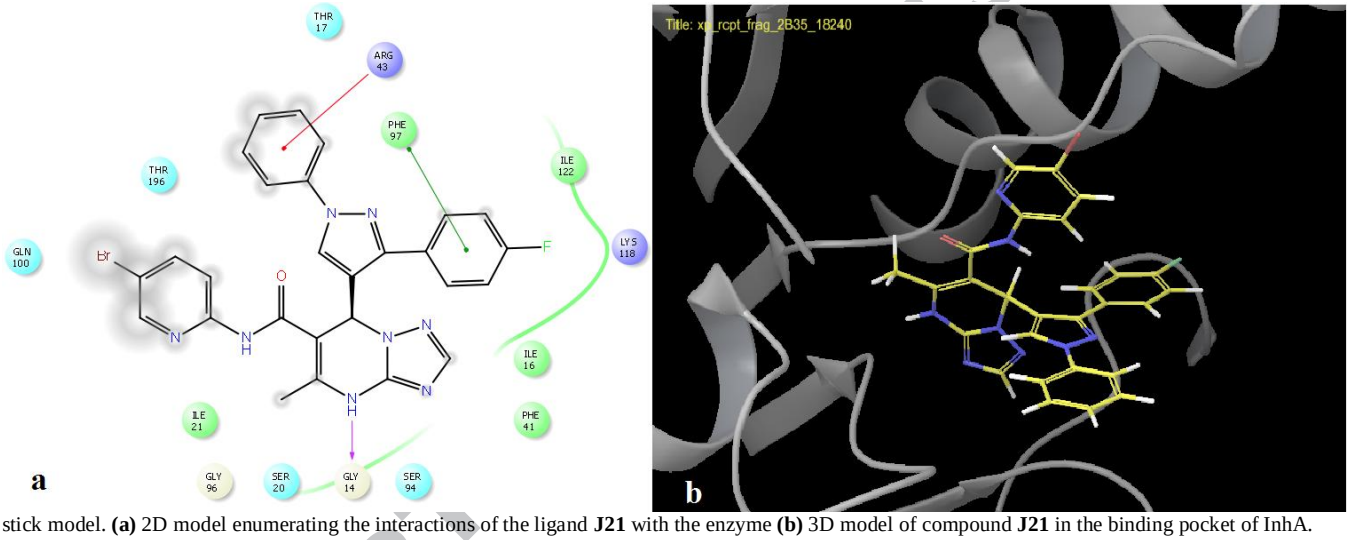

Figure 2: The binding model of docked compound **J27** with enoyl ACP reductase (InhA) enzyme. The enzyme is displayed as cartoon, while the compounds as stick model. **(a)** 2D model enumerating the interactions of the ligand **J27** with the enzyme **(b)** 3D model of compound **J27** in the binding pocket of InhA.

greatly reduced the potency of the compounds. Comparably fluorine substituted entities were found to be most potent owing to high electronegativity and hydrophobicity (**J25** & **J27**). The substitutional changes at *para* position of pyridyl ring of carboxamide side arm also influence the activity pattern, the presence of –Br group greatly increases the potency of the compounds as compared to methyl substituted and unsubstituted pyridyl ring. The position R_3 substituted with methyl group demonstrated better activity as compared to isopropyl substituted motifs, which clearly indicates the effect of increase in chain length and branching leading to downfall of potency.

2.3. Docking Study

Molecular docking studies were performed for the active compounds (**J3, J15, J21, J25 and J27**) against the active site of InhA enzyme (PDB Id: 2B35) structure. The results of the docking study with the docking scores, RMS deviation and energies are as summarized in Table 2. The results clearly demonstrate the significant binding affinities with docking energies ranging from -44.89 kcal mol^{-1} to -56.60 kcal mol^{-1} and the RMS deviation values were observed to fall in range of 2-3 Å which can be considered to be acceptable value of deviation.

Table 2: Glide XP score, binding energies and enzyme inhibition assay of triazolo-pyrimidine hybrids

Compound	Glide XP score	RMS[a] Å	Binding energy (kcal/mol)	IC_{50} Enzyme Inhibition (µg/mL)	CC_{50} VERO cells (µg/mL)	S.I.*
J3	-7.47	2.739	-44.89	0.85 ± 0.042	25	29.41
J15	-7.46	2.271	-56.60	0.28 ± 0.014	25	89.28
J21	-9.07	1.866	-49.48	0.11 ± 0.005	20	181.81
J25	-7.17	1.474	-46.59	0.16 ± 0.008	20	125.00
J27	-9.07	1.509	-46.29	0.11 ± 0.005	20	181.81

RMS[a]: The deviation was calculated considering the Triclosan as reference molecule. Measurement of cytotoxicity in VERO cells: 50% inhibitory concentrations or cytotoxic concentrations (µg/mL), * Selectivity index (*in vitro*): CC_{50} of VERO cells/ IC_{50} of enzyme inhibition.

Table 3: Prediction of Lipinski's rule of 5

Compound	mol_MW (<500 amu)	donorHB (<5)	accptHB (<10)	QPlogPo/w (<5)	PSA Å (70-200)	#rotor	'N' of violations (<2)
J3	529.395	1	4.5	6.305	106.253	2	2
J15	574.392	1	5.5	5.673	150.573	3	3
J21	563.84	1	4.5	6.704	105.642	2	2
J25	468.489	1	4.5	6.152	105.671	2	1
J27	547.385	1	4.5	6.636	97.995	2	2

MW: Molecular Weight; donorHB: Hydrogen Bond Donor; accptHB: Hydrogen Bond Acceptor; QPlogPo/w: Partition Coefficient; PSA: Polar Surface Area; #rotor: Rotatable Bonds; 'N' of violations: Number of Lipinski Rule Violations.

Table 4: ADME prediction of triazolo-pyrimidine hybrids

Compound	Percent Human Oral Absorption* (>80% -high & <25% - poor)	QPPCaco* (<25 poor, >500 great)	QPlogBB* (-3.0 – 1.5)	QPlogKhsa* (-1.5 – 1.5)	QPPMDCK* (<25 poor >500 great)	QPlogS* (-6.5 –5)
J3	87.425	693.605	-0.649	1.50	885.563	-8.52
J15	57.316	103.077	-1.773	1.50	113.023	-8.936
J21	90.073	712.72	-0.467	1.60	2249.327	-9.194
J25	100	760.583	-0.653	1.399	665.543	-8.032
J27	93.707	1016.463	-0.377	1.50	2433.214	-9.01

*Calculated using QikProp v 3.5. Range/recommended values calculated for 95% known drugs.

The Figures 1 and 2 illustrates the binding poses as well as interactions of the compounds **J21** and **J27** with highest docking score. The compound **J21** with binding energy -49.48 kcal mol^{-1} and considerably high XP glide score -9.07, binds with InhA active site forming a hydrogen bond between NH of pyrimidines ring and oxygen of carboxylate group of Gly14 at a distance of 2.17 Å. Further, π-π stacking was observed between the two phenyl rings linked to pyrazole ring with phenyl ring of Phe97 and amine group of Arg43 respectively (Figure 1). Proceedingly, the compound **J27** having low binding energy -46.29 kcal mol^{-1} and high XP glide score -9.07, actively interact with the binding pocket of the enzyme structure in the similar pattern as compound **J21** leading to hydrogen bonding between –NH of pyrimidines ring and oxygen of carboxylate group of Gly14 at a distance of 2.28 Å. Additionally, π-π stacking was observed between the two phenyl rings linked to pyrazole ring with phenyl ring of Phe97 and amine group of Arg43 as summarized in figure 2. The other active compounds (**J3**, **J15** and **J25**) similarly binds to the active binding pocket of InhA by forming significant hydrogen bonding as well as π-π interaction and van der Waals interaction.

2.4. Pharmacokinetic properties prediction

Different pharmacokinetic parameters of the synthesized compounds showing good antitubercular activity were calculated using ADME predictions by Quickprop v4.3. The compounds were preliminarily screened considering the basic parameters of Lipinski's rule of 5. Table 3 shows the results obtained from Quickprop with their permissible range. In general an orally active compound should not have more than 2 violations of the Lipinski rule. The active test compounds in present study were not found violating the rule more than the maximum permissible limits and thus proving their drug likeness properties.

The optimum values of the descriptors, polar surface area and rotatable bonds also have great influence on the oral bioavailability of the drug molecules. The important parameters with their permissible ranges are delineated in Table 4. The optimum value of rotatable bonds (<15) and polar surface area (7-200 Å) holds a great importance on the oral bioavailability of the drug molecules.[13] The active test hybrid triazolopyrimidine derivatives demonstrated results of the descriptors to be in the prescribed range thus owing good bioavailability. Intestinal absorption or permeation is also one of the important factor to be studied in concern with the absorption of the drug molecule, which was further confirmed by predicted Caco-2 cell permeability (QPPCaco), used as model for gut- blood barrier.[14] Caco-2 cell permeability prediction of the test compounds indicates excellent results predicting good intestinal absorption. Further, the test results for QPlogkhsa descriptor of Quickprop indicating the predicted values of human serum albumin binding indicated that test molecules were found to fall in the permissible range (-1.5 to 1.5). Also, the Quickprop descriptor for blood/brain partition coefficient QPlogBB showed reliable prediction for all the test compounds and reference drugs. The cell permeability of the blood brain barrier mimic MDCK cells (QPPMDCK) also displayed reliable results falling in the prescribed range. The aqueous solubility parameter (QPlogS) of the test entities was assessed and the compounds were found to be out laid from the permissible range (-6.5-0.5) indicating slight poor solubility of the test molecules which should be further rectified by utilizing solubility enhancers.

2.5. InhA inhibition assay & Cytotoxicity

The active molecules with lower MIC values and good docking score were further evaluated for InhA inhibitory potency. The results obtained are delineated as IC_{50} values of enzyme inhibition in Table 2. The compounds **J21, J25** as well as **J27** demonstrated good inhibitory potency among screened compounds with IC_{50} value of 0.11, 0.16 and 0.11 µg/mL respectively. This indicates a good agreement between docking experiment and InhA inhibitory activity of the potent entities concluding that the anti-tuberculosis activity of the compounds is due to their enzyme inhibitory potency. The active entities

obtained after preliminary screening were further tested for their cytotoxicity on Vero cell using MTT assay and the results were reproduced as 50% growth inhibitory concentration values or cytotoxicity concentration (CC_{50}) which are as displayed in Table 2. The CC_{50} values of the screened compounds emerged no sign of toxicity up to a concentration of 25 µg/mL thus owing a non toxic nature. The S.I. value indicates that the anti-*tb* potency of the compounds is not attributed due to non-specific activity and cytotoxicity as well.

3. Conclusion

Summing up here with, we report the synthesis, anti-tuberculosis activity, docking study, enzyme inhibition study and ADME prediction of novel pyrazole clubbed triazolo[1,5 *a*]pyrimidine hybrids. The *in vitro* study of the hybrids yielded five potent entities (**J3, J15, J21, J25** and **J27**) owing their potency in micro molar range and further exerting no cytotoxicity against Vero cells. Eventually, docking study of the active entries against InhA enzyme active site was performed to study binding pattern of the active motifs. Compounds **J21** and **J27** were found to show good binding affinity with the active binding site of InhA enzyme with lowest binding energies and comparably high Glide XP scores. Further, the results of enzyme inhibition assay and ADME prediction study provides a confirmation to consider the active molecules as lead targets for further progress in drug discovery process.

4. Experimental

4.1. General Chemistry

All chemicals and solvents were obtained from commercial suppliers and were used without further purification. Melting points were determined on an electro thermal melting point apparatus (Buchi BM530) in open capillary tubes and are uncorrected. All reactions were monitored by thin-layer chromatography (TLC on alluminium plates coated with silica gel 60 F254, 0.25 mm thickness, E. Merck, Mumbai-India) and detection of the components were measured under UV light or explore in Iodine chamber. IR spectra for the compounds were recorded using FTIR Perkin Elmer Spectrum 100 spectrometer as KBr pellets with absorption in cm^{-1}. ^{1}H and ^{13}C NMR measurements were carried out on Avance-II 400 Bruker NMR spectrometer. Chemical shifts are expressed in δ (ppm) relative to tetramethylsilane. Elemental analysis was performed on a Thermo Scientific (FLASH 2000) elemental analyzer. Mass analysis was performed on Waters Micromass Q-Tof Micro, mass spectrometer.

4.1.1. Typical procedure for synthesis of 1,3-diphenyl-1-H-pyrazole-4-carbaldehyde derivatives and pyridin-2-yl-3-oxobutanamide derivatives

The divergent substituted acetoacetanilide derivatives retaining electron donating and electron withdrawing group were synthesized by refluxing corresponding substituted 2-aminopyridine with ethylacetoacetate and methylisobutyrylacetate respectively under microwave irradiation (Scheme S2).[11] Proceedingly, 1,3-diarylpyrazole-4-carbaldehyde derivatives were prepared following a two step protocol involving treatment of corresponding hydrazones formed from various substituted acetophenones and phenylhydrazine by excess Vilsmeier reagent (Scheme S1) as reported by Yadlapalli *et al.*[11]

4.1.2. Typical procedure for synthesis of 7-(1,3-diphenyl-1H-pyrazol-4-yl)-5-methyl-N-(pyridin-2-yl)-4,7-dihydro-[1,2,4]triazolo[1,5-a]pyrimidine-6-carboxamide (J1) and related compounds (J2-J30)

A mixture of the appropriate aldehyde **1** (0.01 mol), aminoazole **2** (0.015 mol) and appropriate acetoacetanilides **3** (0.01 mol) were refluxed in 0.4 mL of DMF[15] for specific time interval as visualized by TLC. After cooling, acetone (~10 mL) was added. The reaction mixture was allowed to stand overnight and then filtered to give the solid triazolopyrimidine products **J1-J30**, which were crystallized from ethanol and subsequently dried in air.

4.2. In Vitro antitubercular activity

All the synthesized compounds were examined for antituberculosis activity against *Mycobacterium tuberculosis* H37Rv (MTCC 300) strain using Lowenstein-Jensen medium method.[16] Isoniazide, Ethambutol and Rifampicin was used as the standard drug. The dilutions of standard drugs were prepared in DMSO to get different concentrations of 0.1-6.25 µg/mL. Stock solutions of synthesized compounds were prepared in DMSO. Further dilutions were prepared in DMSO to get different concentrations 1.0 mL of each concentration was used for the study, to this 9.0 mL of Lowenstein-Jensen medium was added. A sweep from *M. tuberculosis* H37RV strain culture was discharged with the help of Nichrome wire loop having 3 mm external diameter into a vial containing 4 mL of sterile distilled water. The vial was shaken for 5 min. The suspension was inoculated on the surface test compounds containing Lowenstein-Jensen medium. Further test media was incubated for 4 weeks at 37 °C. Readings were taken after incubation period of 4 weeks. Further the activity was determined by measuring the OD at 600 nm followed by the calculating the percentage inhibition.

$$\% \text{ Inhibition} = \frac{OD_{(Blank)} - OD_{(Test)}}{OD_{(Blank)}} \times 100$$

4.3. Cell viability by MTT assay

The determination of the cytotoxicity of the synthesized compounds was determined by MTT assay against Vero cell using Promega CellTiter 96 Non-radioactive Cell Proliferation Assay (Promega, Madison, WI, USA). The cellular viability was assessed on basis of conversion of MTT into formazan by the Vero cells after 72 hours of incubation at 37 °C. Further the activity was determined by measuring the absorbance at 540 nm followed by the calculating the percentage cell viability.[17]

$$\text{Percentage cell viability} = \left[100 - \left(\frac{A_o - A_t}{A_o}\right) \times 100\right]$$

Where, A_o = Absorbance of cells treated with 0.1% DMSO medium, A_t = Absorbance of cells treated with various concentration of the samples.

Each treatment was performed in triplicate and the 50% inhibitory concentration (IC_{50}) of each compound was obtained using the Graph Pad Prism program, version 3 (San Diego, CA).

4.4. Computational studies and ADMET prediction method

The molecular structures of all the compounds were drawn using ChemBioDraw Ultra 14.0 (www.cambridgesoft.com). These structures were then imported into Maestro implemented in Schrödinger, further energy of the 3D structures was minimized using Ligprep 3.3 module. The crystal structure of InhA (PDB ID: 2B35) was extracted from protein data bank (www.rcsb.org). The refining of the protein structure and addition of hydrogen atoms to the structure was accomplished utilizing Protein Preparation Wizard (Maestro 10.1 Schrödinger, LLC, New York, NY, 2015). The binding site in the protein molecules was

predicted using Sitemap 3.4 wizard and further the center of the grid was defined, which was generated using Glide 6.6 (Schrödinger, LLC, New York, NY, 2015) with default settings for all parameters. The grid size was kept sufficiently high so as to include the atoms participating in the interaction and then all the compounds were docked against the grid of prepared receptors (mutant InhA) using Glide in XP (Extra Precession) mode[18] with other default setting for scoring function.

The pharmacokinetic profile of the test compounds showing good antitubercular activity were predicted by using programs Qikprop v4.3 (Schrödinger, Inc., New York, NY, 2015). The compounds prepared by LigPrep 3.3 were utilized for the calculation of pharmacokinetic parameters by QikProp v4.3. The program QikProp v4.3, utilizes the method of Jorgensen[19] to compute pharmacokinetic properties and descriptors.

4.5. Enzyme Inhibition Assay

Spectrophotometric method was utilized to assay the inhibition of Wild type enoyl-ACP reductase (InhA) procured by over expression of gene cloned in pET-28a(+) vector transformed into *E. coli* BL21(DE3) cells as reported by Liu et al.[20a], which was furnished by monitoring the decrease in the absorbance of NADH at 340 nm at 25 °C. The 100 µL standard reaction mixture, contained 150 mM Tris-NaCl buffer (pH 7.5), 200 µM crotonoyl-CoA, 100 µM NADH, 200 nM enzyme, and 1% DMSO. A solution of inhibitors was prepared in DMSO keeping concentration 10mM. A serially diluted stock was added to the final reaction mixture for inhibition studies. The reaction proceeds by reduction of crotonoyl-CoA (Sigma) to butyryl-CoA with the oxidation of NADH to NAD+, which is monitored at 340 nm. The conversion of crotonoyl-CoA to butyryl-CoA is the last step in fatty acid chain elongation step moreover easy availability of crotonoyl-CoA encouraged the use as substrate. Data points were the mean of three different sets of experiments, and the individual values were within ±5% of the average.[20b]

IC_{50} values of the synthesized compounds and Triclosan as positive control against InhA were determined by measuring the activity of the enzyme at various concentrations of these compounds. In the standard reaction mixture mentioned above, various concentrations of the compounds of interest were added one by one, and the percent inhibition was calculated from the residual enzymatic activity. The percent activity thus calculated was plotted against log concentration of the compound. The data were analyzed by nonlinear regression method using SigmaPlot 6.0 and the value of IC_{50} determined from the fit of the data (IC_{50} corresponds to the concentration of the compound that inhibited ENR activity by 50%).[20]

Acknowledgments

We articulate our appreciation to authorities of V. P. & R. P. T. P. Science College, Sardar Patel University, Vallabh Vidyanagar (Gujarat-India) for providing infrastructural & chemical facilities. We forward our gratefulness to DST-Delhi for providing financial aid to the author Jaimin D. Bhatt in form of INSPIRE fellowship (IF120757). The support of Dr. Raghu R. and the team Schrodinger (Bangalore) for Maestro-2015-1 is greatly lauded. We are thankful to the Director SAIF, Chandigarh for spectroscopic analysis facility. The support of Director, SICART, Vallabh Vidyanagar is appreciated for elemental analysis and IR spectroscopy.

Supplementary data

Scheme S1-S2, Table S1, Experimental data and Figure S1-S7 are available in supplementary information.

References and notes

1. Sharma, S. K.; Mohan, A., Tuberculosis: From an incurable scourge to a curable disease-journey over a millennium. *The Indian journal of medical research* **2013,** *137* (3), 455.
2. Snider, D.; Raviglione, M.; Kochi, A.; Bloom, B., Tuberculosis: Pathogenesis. *Protection and Control: Global Burden of Tuberculosis* **1994**, 3.
3. WHO., *Global Tuberculosis Report 2014*. World Health Organization: 2014.
4. Krishna, K. M.; Inturi, B.; Pujar, G. V.; Purohit, M. N.; Vijaykumar, G., Design, synthesis and 3D-QSAR studies of new diphenylamine containing 1, 2, 4-triazoles as potential antitubercular agents. *European journal of medicinal chemistry* **2014,** *84*, 516-529.
5. Janin, Y. L., Antituberculosis drugs: ten years of research. *Bioorganic & medicinal chemistry* **2007,** *15* (7), 2479-2513.
6. Kuo, M. R.; Morbidoni, H. R.; Alland, D.; Sneddon, S. F.; Gourlie, B. B.; Staveski, M. M.; Leonard, M.; Gregory, J. S.; Janjigian, A. D.; Yee, C., Targeting tuberculosis and malaria through inhibition of enoyl reductase compound activity and structural data. *Journal of Biological Chemistry* **2003,** *278* (23), 20851-20859.
7. Saini M. S.; Kumar A.; Dwivedi J.; Singh R.' A REVIEW: Biological significances of heterocyclic compounds. *Int J Pharma Sci and Res* **2013**, *4*, 66- 77.
8. Singh, M.; Fatma, S.; Ankit, P.; Singh, S. B.; Singh, J., Boric acid in aqueous micellar medium: an effective and recyclable catalytic system for the synthesis of aryl-7, 8-dihydro [1, 2, 4] triazolo [4, 3-a] pyrimidine-6-carbonitriles. *Tetrahedron Letters* **2014,** *55* (2), 525-527.
9. El-Gendy, M. M.; Shaaban, M.; Shaaban, K. A.; El-Bondkly, A. M.; Laatsch, H., Essramycin: A First Triazolopyrimidine Antibiotic Isolated from Nature†. *The Journal of antibiotics* **2008,** *61* (3), 149-157.
10. (a) Castagnolo, D.; Manetti, F.; Radi, M.; Bechi, B.; Pagano, M.; De Logu, A.; Meleddu, R.; Saddi, M.; Botta, M., Synthesis, biological evaluation, and SAR study of novel pyrazole analogues as inhibitors of Mycobacterium tuberculosis: Part 2. Synthesis of rigid pyrazolones. *Bioorganic & medicinal chemistry* **2009,** *17* (15), 5716-5721. (b) Kadam, A.; Dawane, B.; Pawar, M.; Shegokar, H.; Patil, K.; Meshram, R.; Gacche, R., Development of novel pyrazolone derivatives as inhibitors of aldose reductase: An eco-friendly one-pot synthesis, experimental screening and in silico analysis. *Bioorganic chemistry* **2014,** *53*, 67-74.
11. (a) Yadlapalli, R. K.; Chourasia, O.; Vemuri, K.; Sritharan, M.; Perali, R. S., Synthesis and in vitro anticancer and antitubercular activity of diarylpyrazole ligated dihydropyrimidines possessing lipophilic carbamoyl group. *Bioorganic & medicinal chemistry letters* **2012,** *22* (8), 2708-2711. (b) Trivedi, A.; Dodiya, D.; Dholariya, B.; Kataria, V.; Bhuva, V.; Shah, V., Synthesis and Biological Evaluation of Some Novel 1, 4-Dihydropyridines as Potential AntiTubercular Agents. *Chemical biology & drug design* **2011,** *78* (5), 881-886.
12. (a) Pregnolato, M.; Terreni, M.; Ubiali, D.; Pagani, G.; Borgna, P.; Pastoni, F.; Zampollo, F., 3H-[1, 2] Dithiolo [3, 4-b] pyridine-3-thione and its derivatives Synthesis and antimicrobial activity. *Il Farmaco* **2000,** *55* (11), 669-679. (b) R.J. Heath, Y.-T. Yu, M.A. Shapiro, E. Olson, C.O. Rock, Broad spectrum antimicrobial biocides target the FabI component of fatty acid synthesis, *Journal of Biological Chemistry* **1998**, 273, 30316-30320.
13. (a) Ivan, D.; Crisan, L.; Pacureanu, L., Docking Experiment for (3S, 5S, 6S)-6-Acetylamidopenicillanic Acid. *REVISTA DE CHIMIE* **2011,** *62* (8), 806-809. (b) Lu, J. J.; Crimin, K.; Goodwin, J. T.; Crivori, P.; Orrenius, C.; Xing, L.; Tandler, P. J.; Vidmar, T. J.; Amore, B. M.; Wilson, A. G., Influence of molecular flexibility and polar surface area metrics on oral bioavailability in the rat. *Journal of medicinal chemistry* **2004,** *47* (24), 6104-6107.
14. Artursson, P.; Palm, K.; Luthman, K., Caco-2 monolayers in experimental and theoretical predictions of drug transport. *Advanced drug delivery reviews* **2012,** *64*, 280-289.
15. Muravyova, E. A.; Desenko, S. M.; Rudenko, R. V.; Shishkina, S. V.; Shishkin, O. V.; Sen'ko, Y. V.; Vashchenko, E. V.; Chebanov, V. A., Switchable selectivity in multicomponent

heterocyclizations of acetoacetamides, aldehydes, and 3-amino-1, 2, 4-triazoles/5-aminopyrazoles. *Tetrahedron* **2011,** *67* (48), 9389-9400.

16. Patel, J.; Dholariya, H.; Patel, K.; Bhatt, J.; Patel, K., Cu (II) and Ni (II) complexes of coumarin derivatives with fourth generation flouroquinolone: synthesis, characterization, microbicidal and antioxidant assay. *Medicinal Chemistry Research* **2014,** *23* (8), 3714-3724.
17. Kong, Y.; Ma, W.; Liu, X.; Zu, Y.; Fu, Y.; Wu, N.; Liang, L.; Yao, L.; Efferth, T., Cytotoxic activity of curcumin towards CCRF-CEM leukemia cells and its effect on DNA damage. *Molecules* **2009,** *14* (12), 5328-5338.
18. Friesner, R. A.; Murphy, R. B.; Repasky, M. P.; Frye, L. L.; Greenwood, J. R.; Halgren, T. A.; Sanschagrin, P. C.; Mainz, D. T., Extra precision glide: docking and scoring incorporating a model of hydrophobic enclosure for protein-ligand complexes. *Journal of medicinal chemistry* **2006,** *49* (21), 6177-6196.
19. Duffy, E. M.; Jorgensen, W. L., Prediction of properties from simulations: free energies of solvation in hexadecane, octanol, and water. *Journal of the American chemical society* **2000,** *122* (12), 2878-2888.
20. (a) Liu, J.; Wu, J.; Li, Z., Enoyl acyl carrier protein reductase (FabI) catalyzed asymmetric reduction of the C [double bond, length as m-dash] C double bond of α, β-unsaturated ketones: preparation of (R)-2-alkyl-cyclopentanones. *Chemical Communications* **2014,** *50* (68), 9729-9732. (b) Kapoor, M.; Dar, M. J.; Surolia, A.; Surolia, N., Kinetic determinants of the interaction of enoyl-ACP reductase from Plasmodium falciparum with its substrates and inhibitors. *Biochemical and biophysical research communications* **2001,** *289* (4), 832-837.